

Effective damping enhancement in noncollinear spin structures

Levente Rózsa,* Julian Hagemeister, Elena Y. Vedmedenko, and Roland Wiesendanger

Department of Physics, University of Hamburg, D-20355 Hamburg, Germany



(Received 30 April 2018; published 14 September 2018)

Damping mechanisms in magnetic systems determine the lifetime, diffusion, and transport properties of magnons, domain walls, magnetic vortices, and skyrmions. Based on the phenomenological Landau-Lifshitz-Gilbert equation, here the effective damping parameter in noncollinear magnetic systems is determined describing the linewidth in resonance experiments or the decay parameter in time-resolved measurements. It is shown how the effective damping can be calculated from the elliptic polarization of magnons, arising due to the noncollinear spin arrangement. It is concluded that the effective damping is larger than the Gilbert damping, and it may significantly differ between excitation modes. Numerical results for the effective damping are presented for the localized magnons in isolated skyrmions, with parameters based on the Pd/Fe/Ir(111) model-type system.

DOI: [10.1103/PhysRevB.98.100404](https://doi.org/10.1103/PhysRevB.98.100404)

Spin waves (SWs) or magnons as elementary excitations of magnetically ordered materials have attracted significant research attention lately. The field of magnonics [1] concerns the creation, propagation, and dissipation of SWs in nanostuctured magnetic materials, where the dispersion relations can be adjusted by the system geometry. A possible alternative for engineering the properties of magnons is offered by noncollinear (NC) spin structures [2] instead of collinear ferromagnets (FMs) or antiferromagnets (AFMs). SWs are envisaged to act as information carriers, where one can take advantage of their low wavelengths compared to electromagnetic waves possessing similar frequencies [3]. Increasing the lifetime and the stability of magnons, primarily determined by the relaxation processes, is of crucial importance in such applications.

The Landau-Lifshitz-Gilbert (LLG) equation [4,5] is commonly applied for the quasiclassical description of SWs, where relaxation is encapsulated in the dimensionless Gilbert damping (GD) parameter α . The lifetime of excitations can be identified with the resonance linewidth in frequency-domain measurements such as ferromagnetic resonance (FMR) [6], Brillouin light scattering [7], or broadband microwave response [8], and with the decay speed of the oscillations in time-resolved experiments including magneto-optical Kerr effect microscopy [9] and scanning transmission x-ray microscopy [10]. Since the linewidth is known to be proportional to the frequency of the magnon, measuring the ratio of these quantities is a widely applied method for determining the GD in FMs [3,6]. An advantage of AFMs in magnonics applications [11,12] is their significantly enhanced SW frequencies due to the exchange interactions, typically in the terahertz regime, compared to FMs with gigahertz frequency excitations. However, it is known that the linewidth in AFM resonance is typically very wide because it scales with a larger effective damping parameter α_{eff} than the GD α [13].

The tuning of the GD can be achieved in magnonic crystals by combining materials with different values of α . It was demonstrated in Refs. [14–16] that this leads to a strongly frequency- and band-dependent α_{eff} , based on the relative weights of the magnon wave functions in the different materials.

Magnetic vortices are two-dimensional NC spin configurations in easy-plane FMs with an out-of-plane magnetized core, constrained by nanostructuring them in dot- or pillar-shaped magnetic samples. The excitation modes of vortices, particularly their translational and gyroscopic modes, have been investigated using collective-coordinate models [17] based on the Thiele equation [18], linearized SW dynamics [19,20], numerical simulations [21], and experimental techniques [22–24]. It was demonstrated theoretically in Ref. [21] that the rotational motion of a rigid vortex excited by spin-polarized current displays a larger α_{eff} than the GD; a similar result was obtained based on calculating the energy dissipation [25]. However, due to the unbounded size of vortices, the frequencies as well as the relaxation rates sensitively depend on the sample preparation, particularly because they are governed by the magnetostatic dipolar interaction.

In magnetic skyrmions [26], the magnetic moment directions wrap the whole unit sphere. In contrast to vortices, isolated skyrmions need not be confined for stabilization, and are generally less susceptible to demagnetization effects [3,27]. The SW excitations of the skyrmion lattice phase have been investigated theoretically [28–30] and subsequently measured in bulk systems [3,8,31]. It was calculated recently [32] that the magnon resonances measured via electron scattering in the skyrmion lattice phase should broaden due to the NC structure. Calculations predicted the presence of different localized modes concentrated on the skyrmion for isolated skyrmions on a collinear background magnetization [33–35] and for skyrmions in confined geometries [20,36,37]. From the experimental side, the motion of magnetic bubbles in a nanodisk was investigated in Ref. [38], and it was proposed recently that the gyration frequencies measured in Ir/Fe/Co/Pt multilayer films are characteristic of a dilute array of isolated

*rozsa.levente@physnet.uni-hamburg.de

skyrmions rather than a well-ordered skyrmion lattice [6]. However, the lifetime of magnons in skyrmionic systems based on the LLG equation is apparently less explored.

It is known that NC spin structures may influence the GD via emergent electromagnetic fields [29,39,40] or via the modified electronic structure [41,42]. Besides determining the SW relaxation process, the GD also plays a crucial role in the motion of domain walls [43–45] and skyrmions [46–48] driven by electric or thermal gradients, both in the Thiele equation where the skyrmions are assumed to be rigid and when internal deformations of the structure are considered. Finally, damping and deformations are also closely connected to the switching mechanisms of superparamagnetic particles [49,50] and vortices [51], as well as the lifetime of skyrmions [52–54].

The α_{eff} in FMs depends on the sample geometry due to the shape anisotropy [13,55,56]. It was demonstrated in Ref. [56] that α_{eff} is determined by a factor describing the ellipticity of the magnon polarization caused by the shape anisotropy. Elliptic precession and GD were also investigated by considering the excitations of magnetic adatoms on a nonmagnetic substrate [57]. The calculation of the eigenmodes in NC systems, e.g., in Refs. [6,20,35], also enables the evaluation of the ellipticity of magnons, but this property apparently has not been connected to the damping so far.

Although different theoretical methods for calculating α_{eff} have been applied to various systems, a general description applicable to all NC structures seems to be lacking. Here it is demonstrated within a phenomenological description of the linearized LLG equation how magnons in NC spin structures relax with a higher effective damping parameter α_{eff} than the GD. A connection between α_{eff} and the ellipticity of magnon polarization forced by the NC spin arrangement is established. The method is illustrated by calculating the excitation frequencies of isolated skyrmions, considering experimentally determined material parameters for the Pd/Fe/Ir(111) model system [58]. It is demonstrated that the different localized modes display different effective damping parameters, with the breathing mode possessing the highest one.

The LLG equation reads

$$\partial_t \mathbf{S} = -\gamma' \mathbf{S} \times \mathbf{B}^{\text{eff}} - \alpha \gamma' \mathbf{S} \times (\mathbf{S} \times \mathbf{B}^{\text{eff}}), \quad (1)$$

with $\mathbf{S} = \mathbf{S}(\mathbf{r})$ the unit-length vector field describing the spin directions in the system, α the GD, and $\gamma' = \frac{1}{1+\alpha^2} \frac{ge}{2m}$ the modified gyromagnetic ratio (with g being the g factor of the electrons, e the elementary charge, and m the electron mass). Equation (1) describes the time evolution of the spins governed by the effective magnetic field $\mathbf{B}^{\text{eff}} = -\frac{1}{\mathcal{M}} \frac{\delta \mathcal{H}}{\delta \mathbf{S}}$, with \mathcal{H} the Hamiltonian or free energy of the system in the continuum description and \mathcal{M} the saturation magnetization.

The spins will follow a damped precession relaxing to a local minimum \mathbf{S}_0 of \mathcal{H} , given by the condition $\mathbf{S}_0 \times \mathbf{B}^{\text{eff}} = \mathbf{0}$. Note that generally the Hamiltonian represents a rugged landscape with several local energy minima, corresponding to, e.g., FM, spin spiral, and skyrmion lattice phases, or single objects such as vortices or isolated skyrmions. The excitations can be determined by switching to a local coordinate system [20,34,47] with the spins along the z direction in the local minimum, $\tilde{\mathbf{S}}_0 = (0, 0, 1)$, and expanding the Hamiltonian in the variables $\beta^{\pm} = \tilde{S}^x \pm i \tilde{S}^y$, introduced analogously to spin

raising and lowering or bosonic creation and annihilation operators in the quantum-mechanical description of magnons [59–61]. The lowest-order approximation is the linearized form of the LLG equation (1),

$$\partial_t \beta^+ = \frac{\gamma'}{\mathcal{M}} (i - \alpha) [(D_0 + D_{\text{nr}}) \beta^+ + D_a \beta^-], \quad (2)$$

$$\partial_t \beta^- = \frac{\gamma'}{\mathcal{M}} (-i - \alpha) [D_a^\dagger \beta^+ + (D_0 - D_{\text{nr}}) \beta^-]. \quad (3)$$

For details of the derivation see the Supplemental Material [62]. The term D_{nr} in Eqs. (2) and (3) is responsible for the nonreciprocity of the SW spectrum [2]. It accounts for the energy difference between magnons propagating in opposite directions in in-plane oriented ultrathin FM films [63,64] with Dzyaloshinsky-Moriya interaction [65,66] and the splitting between clockwise and counterclockwise modes of a single skyrmion [20].

Here we will focus on the effects of the anomalous term [34] D_a , which couples Eqs. (2) and (3) together. Equations (2) and (3) may be rewritten as eigenvalue equations by assuming the time dependence

$$\beta^{\pm}(\mathbf{r}, t) = e^{-i\omega_k t} \beta_k^{\pm}(\mathbf{r}). \quad (4)$$

For $\alpha = 0$, the spins will precess around their equilibrium direction $\tilde{\mathbf{S}}_0$. If the equations are uncoupled, the \tilde{S}^x and \tilde{S}^y variables describe circular polarization, similarly to the Larmor precession of a single spin in an external magnetic field. However, the spins are forced on an elliptic path due to the presence of the anomalous terms.

The effective damping parameter of mode k is defined as

$$\alpha_{k,\text{eff}} = \left| \frac{\text{Im } \omega_k}{\text{Re } \omega_k} \right|, \quad (5)$$

which is the inverse of the figure of merit introduced in Ref. [15]. Equation (5) expresses the fact that $\text{Im } \omega_k$, the linewidth in resonance experiments or decay coefficient in time-resolved measurements, is proportional to the excitation frequency $\text{Re } \omega_k$.

Interestingly, there is a simple analytic expression connecting $\alpha_{k,\text{eff}}$ to the elliptic polarization of the modes at $\alpha = 0$. For $\alpha \ll 1$, the effective damping may be expressed as

$$\begin{aligned} \frac{\alpha_{k,\text{eff}}}{\alpha} &\approx \frac{\int |\beta_k^{-(0)}(\mathbf{r})|^2 + |\beta_k^{+(0)}(\mathbf{r})|^2 d\mathbf{r}}{\int |\beta_k^{-(0)}(\mathbf{r})|^2 - |\beta_k^{+(0)}(\mathbf{r})|^2 d\mathbf{r}} \\ &= \frac{\int a_k^2(\mathbf{r}) + b_k^2(\mathbf{r}) d\mathbf{r}}{\int 2a_k(\mathbf{r})b_k(\mathbf{r}) d\mathbf{r}}, \end{aligned} \quad (6)$$

where the (0) superscript denotes that the eigenvectors $\beta_k^{\pm}(\mathbf{r})$ defined in Eq. (4) were calculated for $\alpha = 0$, while $a_k(\mathbf{r})$ and $b_k(\mathbf{r})$ denote the semimajor and semiminor axes of the ellipse the spin variables $\tilde{S}^x(\mathbf{r})$ and $\tilde{S}^y(\mathbf{r})$ are precessing on in mode k . Details of the derivation are given in the Supplemental Material [62]. Note that an analogous expression for the uniform precession mode in FMs was derived in Ref. [56]. The main conclusion from Eq. (6) is that $\alpha_{k,\text{eff}}$ will depend on the considered SW mode and it is always at least as high as the GD α . Although Eq. (6) was obtained in the limit of low α , numerical calculations indicate that the $\alpha_{k,\text{eff}}/\alpha$ ratio tends

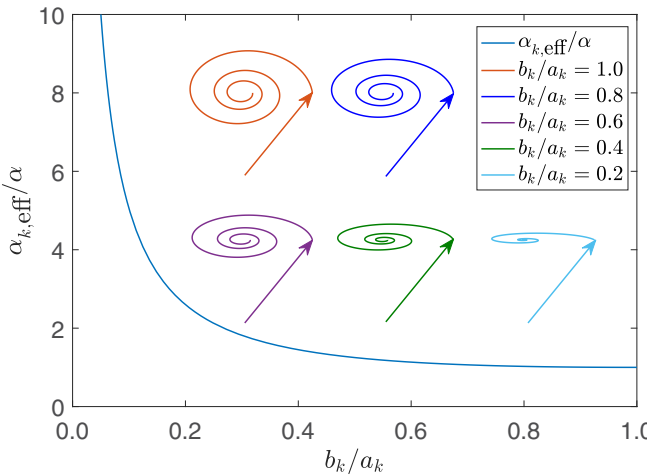


FIG. 1. Effective damping parameter $\alpha_{k,\text{eff}}$ as a function of inverse aspect ratio b_k/a_k of the polarization ellipse, assuming constant a_k and b_k functions in Eq. (6). Insets illustrate the precession for different values of b_k/a_k .

to increase for increasing values of α (see the Supplemental Material [62] for an example). The enhancement of the damping from Eq. (6) is shown in Fig. 1, with the space-dependent $a_k(\mathbf{r})$ and $b_k(\mathbf{r})$ replaced by constants for simplicity. It can be seen that for more distorted polarization ellipses the spins get closer to the equilibrium direction after the same number of precessions, indicating a faster relaxation.

Since the appearance of the anomalous term D_a in Eqs. (2) and (3) forces the spins to precess on an elliptic path, it expresses that the system is not axially symmetric around the local spin directions in the equilibrium state denoted by S_0 . Such a symmetry breaking naturally occurs in any NC spin structure, implying a mode-dependent enhancement of the effective damping parameter in NC systems even within the phenomenological description of the LLG equation. Note that the NC structure also influences the electronic properties of the system, which can lead to a modification of the GD itself (see, e.g., Ref. [42]).

In order to illustrate the enhanced and mode-dependent $\alpha_{k,\text{eff}}$, we calculate the magnons in isolated chiral skyrmions in a two-dimensional ultrathin film. The density of the Hamiltonian \mathcal{H} reads [67]

$$h = \sum_{\alpha=x,y,z} [\mathcal{A}(\nabla S^\alpha)^2] + \mathcal{K}(S^z)^2 - \mathcal{M}BS^z + \mathcal{D}(S^z\partial_x S^x - S^x\partial_x S^z + S^z\partial_y S^y - S^y\partial_y S^z), \quad (7)$$

with \mathcal{A} the exchange stiffness, \mathcal{D} the Dzyaloshinsky-Moriya interaction, \mathcal{K} the anisotropy coefficient, and B the external field.

In the following we will assume $\mathcal{D} > 0$ and $B \geq 0$ without the loss of generality (see the Supplemental Material [62] for discussion). Using cylindrical coordinates (r, φ) in real space and spherical coordinates $S = (\sin \Theta \cos \Phi, \sin \Theta \sin \Phi, \cos \Theta)$ in spin space, the equilibrium profile of the isolated skyrmion will correspond to the cylindrically symmetric configuration $\Theta_0(r, \varphi) = \Theta_0(r)$ and

$\Phi_0(r, \varphi) = \varphi$, the former satisfying

$$\mathcal{A}\left(\partial_r^2 \Theta_0 + \frac{1}{r}\partial_r \Theta_0 - \frac{1}{r^2} \sin \Theta_0 \cos \Theta_0\right) + \mathcal{D}\frac{1}{r} \sin^2 \Theta_0 + \mathcal{K} \sin \Theta_0 \cos \Theta_0 - \frac{1}{2}\mathcal{M}B \sin \Theta_0 = 0 \quad (8)$$

with the boundary conditions $\Theta_0(0) = \pi$, $\Theta_0(\infty) = 0$.

The operators in Eqs. (2) and (3) take the form (cf. Refs. [34,35,47] and the Supplemental Material [62])

$$D_0 = -2\mathcal{A}\left\{\nabla^2 + \frac{1}{2}\left[(\partial_r \Theta_0)^2 - \frac{1}{r^2}(3\cos^2 \Theta_0 - 1)(\partial_\varphi \Phi_0)^2\right]\right\} - \mathcal{D}\left(\partial_r \Theta_0 + \frac{1}{r}3\sin \Theta_0 \cos \Theta_0 \partial_\varphi \Phi_0\right) - \mathcal{K}(3\cos^2 \Theta_0 - 1) + \mathcal{M}B \cos \Theta_0, \quad (9)$$

$$D_{\text{nr}} = \left(4\mathcal{A}\frac{1}{r^2} \cos \Theta_0 \partial_\varphi \Phi_0 - 2\mathcal{D}\frac{1}{r} \sin \Theta_0\right)(-i\partial_\varphi), \quad (10)$$

$$D_a = \mathcal{A}\left[(\partial_r \Theta_0)^2 - \frac{1}{r^2} \sin^2 \Theta_0 (\partial_\varphi \Phi_0)^2\right] + \mathcal{D}\left(\partial_r \Theta_0 - \frac{1}{r} \sin \Theta_0 \cos \Theta_0 \partial_\varphi \Phi_0\right) + \mathcal{K} \sin^2 \Theta_0. \quad (11)$$

Equation (11) demonstrates that the anomalous term D_a responsible for the enhancement of the effective damping can be attributed primarily to the NC arrangement ($\partial_r \Theta_0$ and $\partial_\varphi \Phi_0 \equiv 1$) and secondarily to the spins becoming canted with respect to the global out-of-plane symmetry axis ($\Theta_0 \in \{0, \pi\}$) of the system. The D_{nr} term introduces a nonreciprocity between modes with positive and negative values of the azimuthal quantum number $(-i\partial_\varphi) \rightarrow m$, preferring clockwise rotating modes ($m < 0$) over counterclockwise rotating ones ($m > 0$) following the sign convention of Refs. [20,34]. Because D_0 and D_{nr} depend on m but D_a does not, it is expected that the distortion of the SW polarization ellipse and consequently the effective damping will be more enhanced for smaller values of $|m|$.

The different modes as a function of external field are shown in Fig. 2(a), for the material parameters describing the Pd/Fe/Ir(111) system. The FMR mode at $\omega_{\text{FMR}} = \frac{\gamma}{\mathcal{M}}(\mathcal{M}B - 2\mathcal{K})$, describing a collective in-phase precession of the magnetization of the whole sample, separates the continuum and discrete parts of the spectrum, with the localized excitations of the isolated skyrmion located below the FMR frequency [34,35]. We found a single localized mode for each $m \in \{0, 1, -2, -3, -4, -5\}$ value, so in the following we will denote the excitation modes with the azimuthal quantum number. The $m = -1$ mode corresponds to the translation of the skyrmion on the field-polarized background, which is a zero-frequency Goldstone mode of the system and not shown in the figure. The $m = -2$ mode tends to zero around $B = 0.65$ T, indicating that isolated skyrmions become susceptible to elliptic deformations and subsequently cannot be stabilized at lower field values [68].

The values of $\alpha_{m,\text{eff}}$ calculated from Eq. (6) for the different modes are summarized in Fig. 2(b). It is important to note that for a skyrmion stabilized at a selected field value, the modes

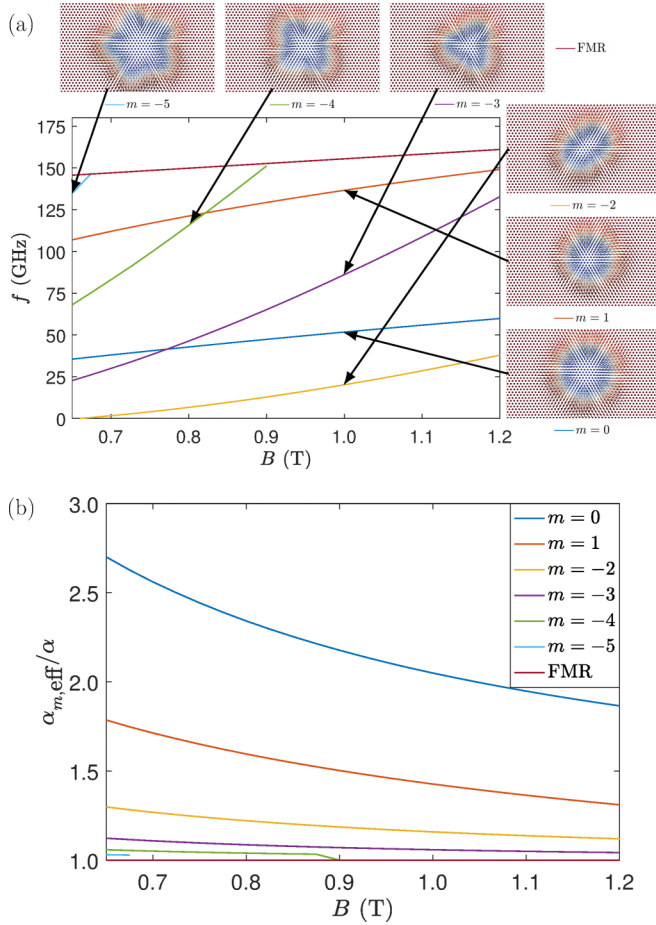


FIG. 2. Localized magnons in the isolated skyrmion, with the interaction parameters corresponding to the Pd/Fe/Ir(111) system [58]: $\mathcal{A} = 2.0 \text{ pJ/m}$, $\mathcal{D} = 3.9 \text{ mJ/m}^2$, $\mathcal{K} = 2.5 \text{ MJ/m}^3$, $\mathcal{M} = 1.1 \text{ MA/m}$. (a) Magnon frequencies $f = \omega/2\pi$ for $\alpha = 0$. Illustrations display the shapes of the excitation modes visualized on the triangular lattice of Fe magnetic moments, with red and blue colors corresponding to positive and negative out-of-plane spin components, respectively. (b) Effective damping coefficients $\alpha_{m,\text{eff}}$, calculated from Eq. (6).

display widely different $\alpha_{m,\text{eff}}$ values, with the breathing mode $m = 0$ being typically damped twice as strongly as the FMR mode. The effective damping tends to increase for lower field values, and decrease for increasing values of $|m|$, the latter property expected from the m dependence of Eqs. (9)–(11) as discussed above. It is worth noting that the $\alpha_{m,\text{eff}}$ parameters are not directly related to the skyrmion size. We also performed the calculations for the parameters describing Ir|Co|Pt multilayers [69], and for the significantly larger skyrmions in that system we obtained considerably smaller excitation frequencies, but quantitatively similar effective damping parameters; details are given in the Supplemental Material [62].

The different effective damping parameters could possibly be determined experimentally by comparing the linewidths of the different excitation modes at a selected field value, or

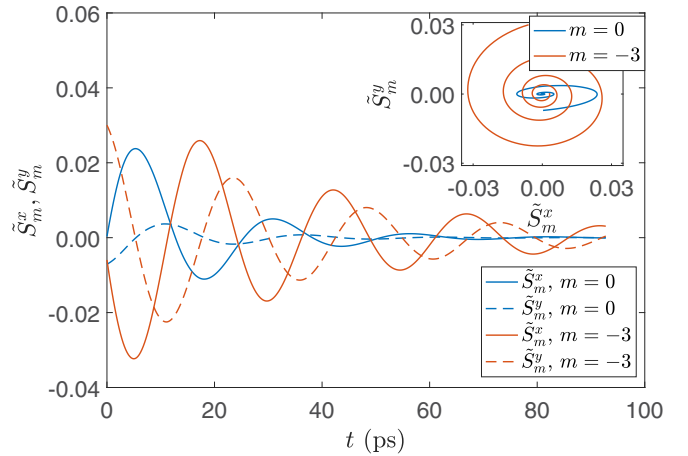


FIG. 3. Precession of a single spin in the skyrmion in the Pd/Fe/Ir(111) system in the $m = 0$ and $m = -3$ modes at $B = 0.75 \text{ T}$, from numerical simulations performed at $\alpha = 0.1$. Inset shows the elliptic precession paths. From fitting the oscillations with Eq. (4), we obtained $|\text{Re } \omega_{m=0}|/2\pi = 39.22 \text{ GHz}$, $|\text{Im } \omega_{m=0}| = 0.0608 \text{ ps}^{-1}$, $\alpha_{m=0,\text{eff}} = 0.25$ and $|\text{Re } \omega_{m=-3}|/2\pi = 40.31 \text{ GHz}$, $|\text{Im } \omega_{m=-3}| = 0.0276 \text{ ps}^{-1}$, $\alpha_{m=-3,\text{eff}} = 0.11$.

investigating the magnon decay over time. An example for the latter case is shown in Fig. 3, displaying the precession of a single spin in the skyrmion, obtained from the numerical solution of the LLG equation (1) with $\alpha = 0.1$. At $B = 0.75 \text{ T}$, the frequencies of the $m = 0$ breathing and $m = -3$ triangular modes are close to each other (cf. Fig. 2), but the former decays much faster. Because in the breathing mode the spin is following a significantly more distorted elliptic path (inset of Fig. 3) than in the triangular mode, the different effective damping is also indicated by Eq. (6).

In summary, it was demonstrated within the phenomenological description of the LLG equation that the effective damping parameter α_{eff} depends on the considered magnon mode. The α_{eff} assumes larger values if the polarization ellipse is strongly distorted as expressed by Eq. (6). Since NC magnetic structures provide an anisotropic environment for the spins, leading to a distortion of the precession path, they represent a natural choice for realizing different α_{eff} values within a single system. The results of the theory were demonstrated for isolated skyrmions with material parameters describing the Pd/Fe/Ir(111) system. The results presented here may stimulate further experimental or theoretical work on the effective damping in skyrmions, vortices, domain walls, or spin spirals.

The authors would like to thank U. Atxitia and G. Meier for fruitful discussions. Financial support by the Alexander von Humboldt Foundation, by the Deutsche Forschungsgemeinschaft via SFB 668, by the European Union via the Horizon 2020 research and innovation program under Grant Agreement No. 665095 (MAGicSky), and by the National Research, Development and Innovation Office of Hungary under Project No. K115575 is gratefully acknowledged.

[1] V. V. Kruglyak, S. O. Demokritov, and D. Grundler, *J. Phys. D: Appl. Phys.* **43**, 264001 (2010).

[2] M. Garst, J. Waizner, and D. Grundler, *J. Phys. D: Appl. Phys.* **50**, 293002 (2017).

- [3] T. Schwarze, J. Waizner, M. Garst, A. Bauer, I. Stasinopoulos, H. Berger, C. Pfleiderer, and D. Grundler, *Nat. Mater.* **14**, 478 (2015).
- [4] L. Landau and E. Lifshitz, *Phys. Z. Sowjetunion* **8**, 153 (1935); *Ukr. J. Phys.* **53**(Special Issue), 14 (2008).
- [5] T. L. Gilbert, *IEEE Trans. Magn.* **40**, 3443 (2004).
- [6] B. Satywal, F. Ma, S. He, M. Raju, V. P. Kravchuk, M. Garst, A. Soumyanarayanan, and C. Panagopoulos, *arXiv:1802.03979*.
- [7] A. A. Serga, S. O. Demokritov, B. Hillebrands, and A. N. Slavin, *Phys. Rev. Lett.* **92**, 117203 (2004).
- [8] Y. Onose, Y. Okamura, S. Seki, S. Ishiwata, and Y. Tokura, *Phys. Rev. Lett.* **109**, 037603 (2012).
- [9] Y. Liu, L. R. Shelford, V. V. Kruglyak, R. J. Hicken, Y. Sakuraba, M. Oogane, Y. Ando, and T. Miyazaki, *J. Appl. Phys.* **101**, 09C106 (2007).
- [10] S. Finizio, S. Wintz, E. Kirk, A. K. Suszka, S. Gliga, P. Wohlhüter, K. Zeissler, and J. Raabe, *Phys. Rev. B* **96**, 054438 (2017).
- [11] K. Abraha, D. E. Brown, T. Dumelow, T. J. Parker, and D. R. Tilley, *Phys. Rev. B* **50**, 6808 (1994).
- [12] R. E. Camley, M. R. F. Jensen, S. A. Feiven, and T. J. Parker, *J. Appl. Phys.* **83**, 6280 (1998).
- [13] A. G. Gurevich and G. A. Melkov, *Magnetization Oscillations and Waves* (CRC Press, Boca Raton, 1996).
- [14] V. V. Kruglyak and A. N. Kuchko, *Phys. Met. Metallogr.* **92**, 211 (2001).
- [15] R. P. Tiwari and D. Stroud, *Phys. Rev. B* **81**, 220403(R) (2010).
- [16] J. Romero Vivas, S. Mamica, M. Krawczyk, and V. V. Kruglyak, *Phys. Rev. B* **86**, 144417 (2012).
- [17] K. Yu. Guslienko, B. A. Ivanov, V. Novosad, Y. Otani, H. Shima, and K. Fukamichi, *J. Appl. Phys.* **91**, 8037 (2002).
- [18] A. A. Thiele, *Phys. Rev. Lett.* **30**, 230 (1973).
- [19] B. A. Ivanov, H. J. Schnitzer, F. G. Mertens, and G. M. Wysin, *Phys. Rev. B* **58**, 8464 (1998).
- [20] M. Mruczkiewicz, P. Gruszecki, M. Krawczyk, and K. Y. Guslienko, *Phys. Rev. B* **97**, 064418 (2018).
- [21] B. Krüger, A. Drews, M. Bolte, U. Merkt, D. Pfannkuche, and G. Meier, *Phys. Rev. B* **76**, 224426 (2007).
- [22] V. Novosad, M. Grimsditch, K. Yu. Guslienko, P. Vavassori, Y. Otani, and S. D. Bader, *Phys. Rev. B* **66**, 052407 (2002).
- [23] K. Yu. Guslienko, X. F. Han, D. J. Keavney, R. Divan, and S. D. Bader, *Phys. Rev. Lett.* **96**, 067205 (2006).
- [24] T. Kamionka, M. Martens, A. Drews, B. Krüger, O. Albrecht, and G. Meier, *Phys. Rev. B* **83**, 224424 (2011).
- [25] A. V. Khvalkovskiy, J. Grollier, A. Dussaux, K. A. Zvezdin, and V. Cros, *Phys. Rev. B* **80**, 140401(R) (2009).
- [26] A. N. Bogdanov and D. A. Yablonskiĭ, *Sov. Phys. JETP* **68**, 101 (1989).
- [27] N. S. Kiselev, A. N. Bogdanov, R. Schäfer, and U. K. Rössler, *J. Phys. D: Appl. Phys.* **44**, 392001 (2011).
- [28] O. Petrova and O. Tchernyshyov, *Phys. Rev. B* **84**, 214433 (2011).
- [29] J. Zang, M. Mostovoy, J. H. Han, and N. Nagaosa, *Phys. Rev. Lett.* **107**, 136804 (2011).
- [30] M. Mochizuki, *Phys. Rev. Lett.* **108**, 017601 (2012).
- [31] D. Ehlers, I. Stasinopoulos, V. Tsurkan, H.-A. Krug von Nidda, T. Fehér, A. Leonov, I. Kézsmárki, D. Grundler, and A. Loidl, *Phys. Rev. B* **94**, 014406 (2016).
- [32] F. J. dos Santos, M. dos Santos Dias, F. S. M. Guimarães, J. Bouaziz, and S. Lounis, *Phys. Rev. B* **97**, 024431 (2018).
- [33] S.-Z. Lin, C. D. Batista, and A. Saxena, *Phys. Rev. B* **89**, 024415 (2014).
- [34] C. Schütte and M. Garst, *Phys. Rev. B* **90**, 094423 (2014).
- [35] V. P. Kravchuk, D. D. Sheka, U. K. Rössler, J. van den Brink, and Yu. Gaididei, *Phys. Rev. B* **97**, 064403 (2018).
- [36] J.-V. Kim, F. Garcia-Sánchez, J. Sampaio, C. Moreau-Luchaire, V. Cros, and A. Fert, *Phys. Rev. B* **90**, 064410 (2014).
- [37] M. Beg, M. Albert, M.-A. Bisotti, D. Cortés-Ortuño, W. Wang, R. Carey, M. Vousden, O. Hovorka, C. Ciccarelli, C. S. Spencer, C. H. Marrows, and H. Fangohr, *Phys. Rev. B* **95**, 014433 (2017).
- [38] F. Büttner, C. Moutafis, M. Schneider, B. Krüger, C. M. Günther, J. Geilhufe, C. v. Korff Schmising, J. Mohanty, B. Pfau, S. Schaffert, A. Bisig, M. Foerster, T. Schulz, C. A. F. Vaz, J. H. Franken, H. J. M. Swagten, M. Kläui, and S. Eisebitt, *Nat. Phys.* **11**, 225 (2015).
- [39] A. Bisig, C. A. Akosa, J.-H. Moon, J. Rhensius, C. Moutafis, A. von Bieren, J. Heidler, G. Kiliani, M. Kammerer, M. Curcic, M. Weigand, T. Tyliszczak, B. Van Waeyenberge, H. Stoll, G. Schütz, K.-J. Lee, A. Manchon, and M. Kläui, *Phys. Rev. Lett.* **117**, 277203 (2016).
- [40] C. A. Akosa, P. B. Ndiaye, and A. Manchon, *Phys. Rev. B* **95**, 054434 (2017).
- [41] C. A. Akosa, I. M. Miron, G. Gaudin, and A. Manchon, *Phys. Rev. B* **93**, 214429 (2016).
- [42] F. Freimuth, S. Blügel, and Y. Mokrousov, *Phys. Rev. B* **96**, 104418 (2017).
- [43] F. Schlickeiser, U. Ritzmann, D. Hinzke, and U. Nowak, *Phys. Rev. Lett.* **113**, 097201 (2014).
- [44] S. Selzer, U. Atxitia, U. Ritzmann, D. Hinzke, and U. Nowak, *Phys. Rev. Lett.* **117**, 107201 (2016).
- [45] H. Y. Yuan, Z. Yuan, K. Xia, and X. R. Wang, *Phys. Rev. B* **94**, 064415 (2016).
- [46] W. Jiang, X. Zhang, G. Yu, W. Zhang, X. Wang, M. B. Jungfleisch, J. E. Pearson, X. Cheng, O. Heinonen, K. L. Wang, Y. Zhou, A. Hoffmann, and S. G. E. te Velthuis, *Nat. Phys.* **13**, 162 (2017).
- [47] S.-Z. Lin, *Phys. Rev. B* **96**, 014407 (2017).
- [48] U. Ritzmann, S. von Malottki, J.-V. Kim, S. Heinze, J. Sinova, and B. Dupé, *Nat. Electron.* **1**, 451 (2018).
- [49] W. F. Brown, Jr., *Phys. Rev.* **130**, 1677 (1963).
- [50] W. T. Coffey and Y. P. Kalmykov, *J. Appl. Phys.* **112**, 121301 (2012).
- [51] M. Martens, T. Kamionka, M. Weigand, H. Stoll, T. Tyliszczak, and G. Meier, *Phys. Rev. B* **87**, 054426 (2013).
- [52] J. Hagemeister, N. Romming, K. von Bergmann, E. Y. Vedmedenko, and R. Wiesendanger, *Nat. Commun.* **6**, 8455 (2015).
- [53] L. Rózsa, E. Simon, K. Palotás, L. Udvardi, and L. Szunyogh, *Phys. Rev. B* **93**, 024417 (2016).
- [54] P. F. Bessarab, G. P. Müller, I. S. Lobanov, F. N. Rybakov, N. S. Kiselev, H. Jónsson, V. M. Uzdin, S. Blügel, L. Bergqvist, and A. Delin, *Sci. Rep.* **8**, 3433 (2018).
- [55] S. S. Kalarickal, P. Krivosik, M. Wu, C. E. Patton, M. L. Schneider, P. Kabos, T. J. Silva, and J. P. Nibarger, *J. Appl. Phys.* **99**, 093909 (2006).
- [56] V. Kambersky and C. E. Patton, *Phys. Rev. B* **11**, 2668 (1975).

- [57] F. S. M. Guimarães, M. dos Santos Dias, B. Schwegflinghaus, and S. Lounis, *Phys. Rev. B* **96**, 144401 (2017).
- [58] N. Romming, A. Kubetzka, C. Hanneken, K. von Bergmann, and R. Wiesendanger, *Phys. Rev. Lett.* **114**, 177203 (2015).
- [59] T. Holstein and H. Primakoff, *Phys. Rev.* **58**, 1098 (1940).
- [60] F. J. Dyson, *Phys. Rev.* **102**, 1217 (1956).
- [61] S. V. Maleev, Sov. Phys. JETP **6**, 776 (1958).
- [62] See Supplemental Material at <http://link.aps.org/supplemental/10.1103/PhysRevB.98.100404> for the derivation of the effective damping parameter as well as for the details of the numerical calculations and simulations, including Refs. [70–72].
- [63] L. Udvardi and L. Szunyogh, *Phys. Rev. Lett.* **102**, 207204 (2009).
- [64] K. Zakeri, Y. Zhang, J. Prokop, T.-H. Chuang, N. Sakr, W. X. Tang, and J. Kirschner, *Phys. Rev. Lett.* **104**, 137203 (2010).
- [65] I. Dzyaloshinsky, *J. Phys. Chem. Solids* **4**, 241 (1958).
- [66] T. Moriya, *Phys. Rev. Lett.* **4**, 228 (1960).
- [67] A. Bogdanov and A. Hubert, *J. Magn. Magn. Mater.* **138**, 255 (1994).
- [68] A. Bogdanov and A. Hubert, *Phys. Status Solidi B* **186**, 527 (1994).
- [69] C. Moreau-Luchaire, C. Moutafis, N. Reyren, J. Sampaio, C. A. F. Vaz, N. Van Horne, K. Bouzehouane, K. Garcia, C. Deranlot, P. Wernicke, P. Wohlhüter, J.-M. George, M. Weigand, J. Raabe, V. Cros, and A. Fert, *Nat. Nanotechnol.* **11**, 444 (2016).
- [70] F. Romá, L. F. Cugliandolo, and G. S. Lozano, *Phys. Rev. E* **90**, 023203 (2014).
- [71] A. O. Leonov, T. L. Monchesky, N. Romming, A. Kubetzka, A. N. Bogdanov, and R. Wiesendanger, *New J. Phys.* **18**, 065003 (2016).
- [72] J. Hagemeister, A. Siemens, L. Rózsa, E. Y. Vedmedenko, and R. Wiesendanger, *Phys. Rev. B* **97**, 174436 (2018).